Proceedings of ASME Turbo Expo 2019:
Turbomachinery Technical Conference and Exposition
GT2019
June 17-21, 2019, Phoenix, Arizona, USA

GT2019-90534

TESTING PROPELLER TIP MODIFICATIONS TO REDUCE ACOUSTIC NOISE GENERATION ON A QUADCOPTER PROPELLER

Kenneth Van Treuren
Baylor University
Waco, TX, USA

Charles Wisniewski[1]
Wisniewski Enterprises
USAF Academy, CO, USA

ABSTRACT

Electric propulsion is gaining popularity with over 100 electrically propelled aircraft in development worldwide. There is a growing interest in vertical lift vehicles either for package delivery or for urban air taxis. If these vehicles are to operate near population centers, they must be both quiet and efficient. The goal of this research is to develop a propeller that is more efficient and generates less noise than a stock DJI Phantom 2 quadcopter propeller. Since a large contribution of near field noise generation for a propeller comes from the tip vortex, reducing or minimizing this generated tip vortex was the main objective. After studying the literature on aircraft wing tip vortices and techniques proposed to minimize the wing tip vortex, seven promising tip treatments were selected and applied to a stock DJI Phantom 2 propeller in an attempt to reduce the tip vortex, and, thus, the generated noise. These tip treatments were: 1. Leading Edge Notch, 2. Trailing Edge Notch, 3. Hole, 4. Vortex Generators, 5. Tip Thread, 6. Trailing Edge Sawtooth, and 7. Reverse Half-Delta.

An optimum design would be one that reduces near field noise while at the same time minimizes any additional required power. Several different configurations were tested for each tip treatment to determine the RPM and required power to hold 0.7 lb_f thrust, which simulated a static hover condition. For each test, a radial traverse one inch behind the propeller permitted the measurement of the Sound Pressure Level (SPL) to find the maximum SPL and its radial location. Several configurations tested resulted in 8-10 dBA reductions in SPL when compared to the stock propeller, however, these configurations also resulted in an unacceptable increase in the power required to achieve the desired thrust. Thus, in these cases a decrease in SPL comes at the expense of power, a tradeoff that must be considered for any propeller modification.

The most promising tip treatment tested was the Trailing Edge Notch at a radial location of 0.95 r/R with a Double Slot width and a Double Depth (DSDD). The DSDD configuration as tested reduced the SPL 7.2 dBA with an increase in power required of only 3.96% over the stock propeller. This tradeoff, while not the largest reduction in noise generation measured, seems to be an acceptable power increase for the decrease in SPL achieved. Smoke visualization confirms that the tip vortex is minimized for this configuration.

KEYWORDS: UAS propeller, propeller acoustics, tip vortex, propeller tip treatments

INTRODUCTION

Unmanned Aircraft Systems (UASs) continue to capture the imagination of the public. UASs are generally defined as powered aerial vehicles which sustain flight and are guided without a crew onboard. The name UAS emphasizes the systems nature of the vehicle which includes the unmanned aircraft, the control system, and communications or telemetry link. UAS military applications focus on the intelligence, surveillance, and reconnaissance (ISR) mission. This role is rapidly growing. In the urban environment, UASs perform tasks such as package delivery, and in the future, urban transportation. Operating in the urban environment requires both efficiency and a reduction in generated noise. Power is a limited resource on a UAS and power consumption must be minimized. Reducing the drag of the

[1] The United States Government retains, and by accepting the article for publication, the publisher acknowledges that the United States Government retains, a non-exclusive, paid-up, irrevocable, worldwide license to publish or reproduce the published form of this work, or allow others to do so, for United States Government purposes.

vehicle or improving propulsion system efficiency leads to less power required for flight resulting in a longer endurance. At the same time, an emphasis on reducing the noise of the propulsion system will enhance survivability for the ISR scenario but may require additional power, reducing loiter time. Reducing noise is vital for an ISR application and to allow UASs to coexist with people in the urban environment.

Electric propulsion will be a significant factor in future aircraft design. Almost 100 electrically propelled aircraft are in development worldwide, more than half have appeared since 2017 [1] either in the form of an electric fan and motor to power large commercial aircraft or smaller electric motors and propellers on UASs and quadcopters. NASA is one of the leaders in electric propulsion. They propose a hybrid system to power a large commercial airliner, which they claim should result in a 7-12 % improvement in fuel efficiency [2]. Hybrid systems are also being considered for small UASs as well. The NASA Leading Edge Asynchronous Propeller Technology (LEAPTech) project demonstrated a distributed propulsion system using 18 small UAS style propellers powered by electric motors and lithium iron phosphate batteries [3]. New concepts for air taxis are similar in design to a quadcopter. Germany's 18-rotor Volocopter is already flying in Dubai [4]. Unmanned Aerial Systems, predominantly powered by batteries and small electric motors, are more common today because of their flexibility in accomplishing variety of tasks. ISR is one of the most important missions of UASs in the military however, resupply is also developing into an emerging mission for UASs. Civil and commercial sectors' use of UASs is growing with worldwide applications in industrial, governmental, personal, and recreational use. It is projected that UAS industry will generate $82 billion by 2025 [5].

By far, the most common UAS seems to be the quadcopter (see Fig. 1), with four propellers that control the motion of the machine by spinning in various combinations of direction and speed [7]. Quadcopter size ranges from large manned and cargo carrying quadcopters to very small UASs that could fit in the palm of a hand. Quadcopters have their limitations, the most obvious being the duration of a quadcopter's flight is limited by the available power, typically provided by batteries. Batteries can be heavy and restrict flights to an hour or less, usually under 25 minutes for common quadcopters such as the DJI Phantom 2. If quadcopters are to be successful, batteries (energy density) must improve.

Quadcopter propellers is an emerging research area as propellers seem to be the propulsion system of choice for quadcopters and urban eVTOL systems [8-17]. It is desirable for quadcopter propellers to be efficient, reducing power consumption and maximizing time of operation. Carvalho showed theoretically that a propeller could be designed using more efficient airfoils than currently found on the stock quadcopter resulting in a 30% improvement in efficiency and an 8.9% reduction in power consumption. He did not experimentally test this prediction [18]. Nelson tested 24 simple modifications to this class of propellers to determine which modifications might improve propeller performance. He showed that leading edge notches and Gurney flap modifications improved thrust while both also improved cruise efficiency [19].

FIGURE 1 DJI PHANTOM 2 QUADCOPTER [6]

Most studies of UAS propellers do not address noise generation. Noise generation must be included during the design process if the quadcopter is to operate in a populated/urban environment or used for ISR. The DJI Phantom 2 quadcopter provided the platform for this research effort. Seven tip treatments used on aircraft wings to reduce or eliminate the wing tip vortex were applied to the stock DJI Phantom 2 propeller seeking to lower generated noise. These simple modifications to the stock propeller promised to provide a reduction in noise generation but the cost in power for each tip treatment needed to be quantified.

PROPELLER TESTING

Multiple Propeller Testing

In the literature there is little data on noise generation of the whole UASs or on multiple propellers in close proximity, such as occurs on quadcopters. Kloet et al. tested a small quadcopter in hover outside in a field and measured the sound produced with distance from the quadcopter for several heights [20]. They found that sound did not change significantly around the periphery of the quadcopter on the plane of the propellers. However, they did find that underneath the quadcopter at an angle of 45° the sound could vary by as much as 10 dBA. Also of note was that the decay in sound with distance from the quadcopter generally followed predicted levels of a 6 dBA drop with a doubling of the distance. Two additional

papers have addressed the interaction between propellers such as would be found on a quadcopter. Zhou et al. investigated rotor-to-rotor interactions of small UAV propellers [21]. They mapped the flow field around the propeller using Particle Image Velocimetry (PIV) showing the vorticity at the tip of the propeller. Separation distance between propellers had little effect on the thrust coefficient but closer spacings caused thrust fluctuations 2.5 times larger than the baseline and a noise enhancement of 3 dBA. Zhou and Fattah looked at tonal noise of two small-scale propellers [22] such as would be found on quadcopters. There was little difference in the noise characteristics of a single propeller compared to that of two propellers in close proximity. The dominant frequency in both cases was the blade passing frequency. Two propellers co-rotating have a 3 dBA increase over the single propeller and two propellers counter-rotating have a 5 dBA increase. They found that the phase angle between the two propellers is the most significant factor and can affect the noise from the two propellers by 10 dBA. All agree that more testing is needed.

Single Static Propeller Testing

More recently, interest has turned to static testing of propeller blades, the condition that would be found with quadcopters in hover. Deters et al. [23] statically tested motors and propellers found on a number of commercial UAVs. Testing included third party replacement propellers which were compared with the stock equipment. Their goal was to develop a database for performance of such systems but no notice was given to the noise produced. Deters et al. [24] then proceeded to test motors and propellers for nano, micro, and mini quadrotors to also develop a database for performance. Again no attention was given to the noise produced by these vehicles.

Interest in the noise produced by UAS propellers has been documented in the literature in an attempt to understand the mechanisms which cause the noise. For example, Sinabaldi and Marino [25] characterized two UAS propellers, optimizing the second to reduce the noise signature by as much as 10 dBA on some angular measurements. Leslie et al [26, 27] also characterized propeller tonal noise by examining the laminar boundary layer and transition location on a UAS propeller. They proposed the use of boundary layer trips to reduce tonal noise. Unfortunately no data was given on power consumption in each case. Van Treuren et al. [28] studied quadcopter propellers and determined that the tip vortex was a primary source of near field noise.

Of interest to the aerospace industry is the documentation of the formation of the tip vortex, found either on the tip of a wing or the tip of the propeller [29-39]. Jacuquin [29] described the decay of the vortex behind the aircraft in an attempt to express the impact of the vortex on aircraft flight. Karakus et al. [30] expressed the flow field physics of the formation of the wing tip vortex, seeking to understand the influence of the vortex on induced drag. Computational models are constantly being improved by the introduction of new turbulence equations to more adequately explain the formation of the near field wing tip vortex formation [33]. Effects of freestream turbulence on wing tip vortex formation is also of interest [36] as freestream turbulence was found to change the shape of the vortex structure. The aviation industry seeks to minimize wing tip vortices for safety reasons and to reduce the induced drag saving fuel costs. This can be accomplished through passive or active systems [37] or by influencing the formation of the vortex with different wing tip devices [38, 39].

Focus on Tip Vortex Minimization

Van Treuren et al. [16], Wisniewski et al. [17], and Van Treuren et al. [28] have tested stock and custom propellers typical of those used on quadcopters, namely the DJI Phantom 2. They documented a static hover condition to include noise generation as well as power consumption. Their studies examined methods to reduce the propeller tip vortex in an effort to reduce overall near field propeller noise. This tip vortex is well documented and they have had some initial success in minimizing the tip vortex strength using a leading edge notch. This resulted in a 7 dBA drop in noise production for an increase in power of 14% for the same hover thrust. These results encouraged the prospect for optimizing this design.

Proposed Modifications to the DJI Phantom 2 Quadcopter Stock Propeller

The focus of this study was to reduce the acoustic signature of the stock DJI Phantom 2 quadcopter propeller while at the same time increasing efficiency. The approach taken was to review the literature to identify promising wing tip modifications used with aircraft and then apply these to the DJI Phantom 2 stock propeller. Careful study led to the selection of the following tip treatments:

1. Leading Edge (LE) Notch
2. Trailing Edge (TE) Notch
3. Hole
4. Vortex Generators (VG)
5. Tip Thread
6. Trailing Edge Sawtooth
7. Reverse Half-Delta

EXPERIMENTAL SETUP AND PROCEDURE

USAF Academy Wind Tunnel

The DJI Phantom 2 quadcopter is a typical drone which served as the model for these experiments, using the DJI motors and propellers for testing (see Fig. 1). The stock DJI propeller is a 9.4 x 5.0 meaning the diameter is 9.4

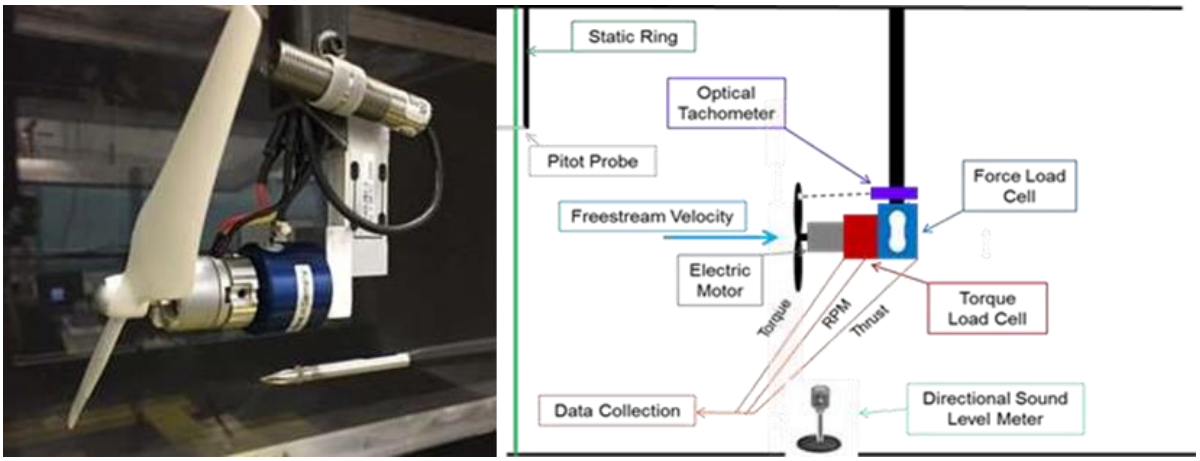

FIGURE 2 PROPELLER AND MOTOR MOUNTED ON TEST RIG [20]

inches (23.88 cm) and the pitch is 5 inches (12.70 cm). Both the wind tunnel and test stand were previously described by Wisniewski et. al. [15]. All tests were accomplished in the North Low-Speed Wind Tunnel (LSWT) at the USAF Academy. This tunnel is an Engineering Design Laboratory, Inc. tunnel with a test section of 36" x 36" x 40" (91.44 cm x 91.4 cm x 101.60 cm) that has a top speed of approximately 108 ft/sec (32.92 m/s). Current tests were conducted under static conditions. Due to the size of the test section and the diameter of the propellers tested, no wind tunnel corrections were needed for the data analysis.

Propeller and Test Rig

The test rig used in the measurement of propeller performance is seen in Fig. 2. The motor used for testing was a 960 Kv brushless motor that was purchased as a slight upgrade to the original DJI Phantom 2 motor. Power for the motor was supplied by a Sorensen SGA40x125C DC Power supply (0 to 40 V, 0 to 125A). The voltage was measured directly and the current was measured with a POWERTEK CTH/50/10/SC/24 VDC which has a range of 0 to 50 ADC. Measurements for the power were made immediately after the power supply and before the motor controller. Control for the motor was accomplished using a standard FUTABA R/C model system which operated a Phoenix ICE2 motor controller.

Instrumentation

The thrust was measured using an Interface MBI-5 thrust transducer capable of a 0 to 2.27 kg_f (0 to 5 lb_f) measurement. Propeller torque was measured with an Interface TS21-2 torque transducer capable of measuring 0 to 2 Nm (0 to 17.7 inch-lb_f). The thrust and torque load cells were calibrated by hanging known weights in line with each of the load cells.

To measure the propeller rotational speed, an OMEGA Remote Optical Sensor, model HHT-20 ROS, was used.

All data were recorded using an Agilent 1421B VXI mainframe with an EC 1431C 64-Channel Scanning A/D card as well as an EC1415A Closed Loop Controller card.

The Brüel & Kjær (B&K) 1/4" microphone used for these tests and was connected to a B&K 2270 Sound Level Meter capable of measuring 20 to 140 dBA with an accuracy of +/- 0.2 dBA and calibrated with a B&K Type 4231 calibration system. The dBA weighting system is used because it more closely resembles the manner the human ear hears. The measurement is a linearly averaged signal over a frequency range of 5 Hz to 24k Hz. The result is a time averaged SPL. The microphone was operated with the nose cone (bullet shape) cover as shown in Fig. 2. Acoustic measurements made in the wind tunnel were only near field and made directly behind the propeller for this study.

For RPM sweeps, the propeller was tested at rotational speeds from 1,500 to 6,500 RPM in 300 RPM increments. During every run, the Sound Pressure Levels (SPL) were recorded and evaluated by logging the SPL of the static wind tunnel prior to activating the propeller and subtracting that value from the measured value recorded during testing to obtain a corrected noise value as seen in Equation 1. All testing was done statically to simulate static hover conditions for a quadcopter.

$$Noise_{\ Corr} = 10 * (\log_{10}(10^{\frac{SPL}{10}} - 10^{\frac{Clean\ SPL}{10}})) \qquad (1)$$

UNCERTAINTY ANALYSIS

The uncertainties of all of the calculated results described in the above procedures were determined using the root-sum-square uncertainty method from Kline and McClintock [40]. The sound pressure level uncertainty

TABLE 1 LE NOTCH CONFIGURATIONS AND DATA – TESTED AT 0.7 Lb_F

Description	Notch Width	Notch Depth	Notch location	Rotational Speed	Mechanical Power	Peak SPL	Peak SPL Location	SPL decrease	Power increase
	(in)	*(in)*	*r/R (%)*	*(RPM)*	*(W)*	*(dBA)*	*r/R (%)*	*(dBA)*	*(%)*
LE_SSSD_75	0.06	0.08	0.75	5903	28.9	117.2	0.85	0.4	2.00
LE_SSDD_75	0.06	0.16	0.75	5930	32.6	115.6	0.81	2.0	10.50
LE_SSDD_87	0.06	0.16	0.87	5923	30.3	116.8	0.83	0.7	2.70
LE_DSDD_87	0.12	0.16	0.87	6087	36.5	110.8	0.77	6.8	23.70
LE_DSDD_90	0.12	0.16	0.9	6148	41.7	110.1	0.74	7.5	41.40
LE_SSSD_95	0.06	0.08	0.95	5809	31.9	117	0.81	0.6	8.10
LE_DSDD_95	0.12	0.08	0.95	6059	35.7	110.4	0.77	7.2	21
LE_DSDD_100	0.12	0.16	1	5986	39.2	112.7	no data	4.9	32.9
Stock				5895	29.5	117.6	0.85		

was estimated to be 0.61 dBA or 0.71% which was nearly entirely attributed to the 0.55 dBA accuracy of the microphone sound level calibrator (General Radio type 1562A). In practice the repeatability of the SPL measurements was ~0.2 dBA. Using Kline and McClintock resulted in an uncertainty in thrust of ± 0.0008 lb_f, in RPM of ± 0.333 RPM, and a torque uncertainty of +/- 0.0011 in-lb_f.

TESTING TIP TREATMENTS

Seven tip treatments were studied. All tip treatments were found by examining the literature for applications to counter wing tip vortices. The goal was to minimize the vortex strength generated at the tip of a stock DJI Phantom 2 quadcopter propeller. Each treatment tested was compared to the stock propeller. The tip treatments were tested under the test condition of 0.7 lb_f of thrust, the thrust required by one propeller when the DJI Phantom 2 was in hover. For each configuration tested, an RPM sweep was first made to determine the exact RPM required for 0.7 lb_f of thrust. Then, at that RPM, a microphone traverse was made at 1 inch behind the trailing edge of the propeller measured at r/R = 0.8. The traverse started 1.5 inches from the centerline near the hub and moved to the tip of the propeller. Again, only near field acoustic measurements were made for this study. This data was used to compare SPL levels for each tip treatment to include the location and magnitude of the maximum SPL. In addition, the mechanical power required to generate 0.7 lb_f of thrust was recorded to compare any changes in the power requirements for the different tip treatments. A summary of each tip treatment will be given as well as an evaluation of the best results from each tip treatment configuration category.

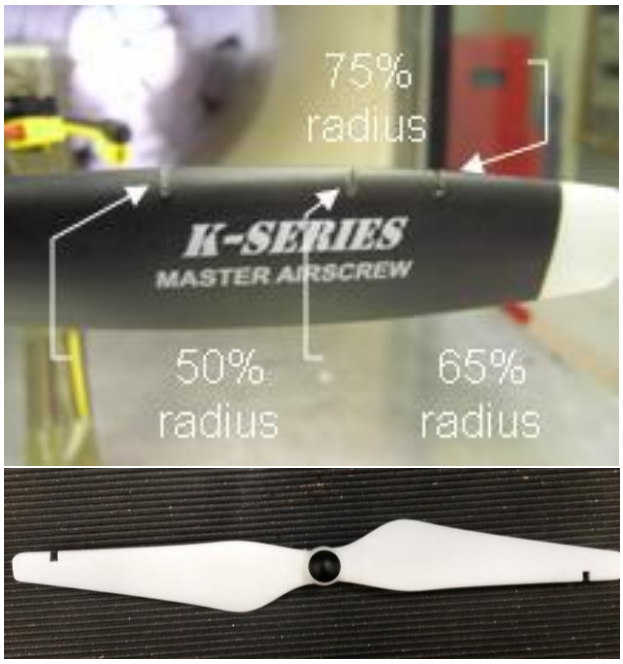

FIGURE 3 TOP- NELSON LEADING EDGE NOTCH [19]; BOTTOM – DSDD DJI PHANTOM 2 LEADING EDGE NOTCH CONFIGURATION

1. Leading Edge Notches

Nelson presented the performance of a leading edge [LE] notch on a typical small fixed-wing UAS propeller [19], shown in Fig. 3. He tested 24 simple modifications to this class of propellers to determine which modifications might improve propeller performance. The results of his tests showed that a leading edge notch at the 0.75 r/R location had a small improvement in performance. At a cruise condition he also showed there was a small improvement in efficiency. These experiments were only concerned with propeller performance and did not address noise generation. More recently Van Treuren et al. [28]

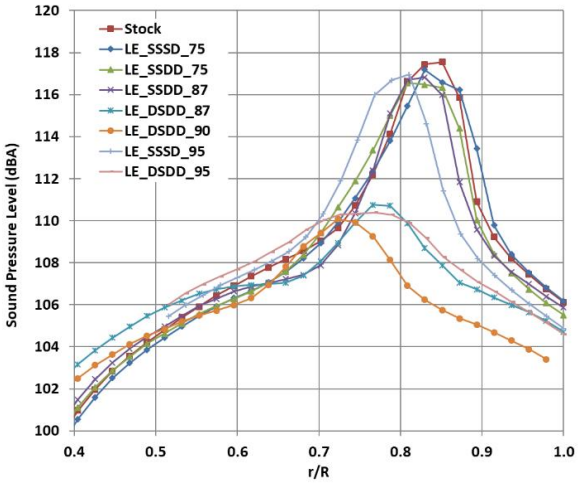

FIGURE 4 SPL VS r/R COMPARISON FOR LE NOTCHES – 1 INCH TRAVERSE

applied LE notches to a stock DJI Phantom 2 quadcopter propeller, also shown in Fig. 3. They tested two locations, r/R of 0.75 (like Nelson) and 0.87. While an improvement in thrust was not found, as suggested by Nelson, there was a 7 dBA reduction in peak SPL with a 14% increase in power required to achieve 0.7 lb_f of thrust. Smoke visualization confirmed that the LE notch did in fact reduce the strength of the tip vortex and its influence downstream. Demoret and Wisniewski [41] continued to test the LE notch at locations of r/R 0.87, 0.90, and 1.00. Further testing was done at a location of r/R = 0.95 in an effort to optimize this tip treatment.

For the LE notch, different slot widths and depths were examined. These widths and depths are listed below along with their abbreviation:

1. Single Slot width (SS)– 0.06 inch wide
2. Double Slot width (DS) – 0.12 inches wide
3. Single Depth (SD)– 0.08 inches deep
4. Double Depth (DD) – 0.16 inches deep

Table 1 lists the configurations tested and the data collected for each configuration compared to the stock propeller.

The RPM and mechanical power are found from the RPM sweeps which were then curve fit to determine the expected RPM value at the thrust required. This standardized the RPM and mechanical power for comparison between the different tip treatments. The RPM found from the sweep then became the target RPM to produce 0.7 lb_f of thrust for the SPL traverse measurements. Using the traverse data, power measurements were compared with the expected value to verify the accuracy of the curve fit. This procedure was used for all tests. Figure 4 shows the 1 inch traverse data for all LE notch configurations tested. The location of the peak SPL tends slightly toward the hub as LE notches are introduced to the propeller.

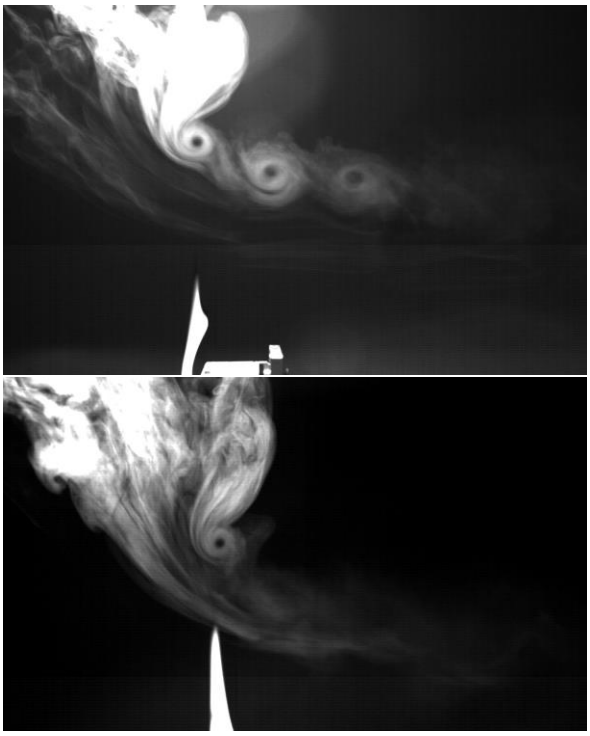

FIGURE 5 DEVELOPMENT OF TIP VORTICIES AND THE SHEAR LAYER ON THE STOCK (TOP)) PROPELLER AND THE LE NOTCH (BOTTOM) [28]

Table 1 shows that moving from a Single Slot width (SS) to a Double Slot width (DS) typically decreases the SPL but increases power required. Also, changing the configuration from a Single Depth (SD) to a Double Depth (DD) also decreases SPL but increases power required. Any increase in power required is seen as an increase in RPM to achieve the desired thrust. While an r/R of 0.9 decreases the SPL 7.5 dBA, the most of any LE notch, it also requires the most power, a 41.40 % increase over the stock propeller. This is clearly unacceptable but illustrates that if the goal is to decrease SPL, then a tradeoff between SPL and power may be required for an acceptable design solution. Ideally it would be desired to decrease SPL with a decrease in power required, however, any modification of the stock propeller typically results in more drag being produced, an increase in RPM required for 0.7 lb_f thrust, and a corresponding increase in power required. ***A better choice might be r/R 0.95 DSDD. This would result in 7.2 dBA decrease in SPL for a power required of 21.0 % more than the stock propeller.***

Figure 5 shows the smoke visualization of the vortex generation at the propeller tip. For the stock propeller, shown in the top of Figure 5, a strong vortex is generated that remains clearly visible downstream of the passing propeller blade. Contrast this with the LE notch which

Table 2 TE Notch Configurations and Data - Tested at 0.7 lb_f

Description	Notch Width	Notch Depth	Notch location	Rotational Speed	Mechanical Power	Peak SPL	Peak SPL Location	SPL decrease	Power increase
	(in)	*(in)*	*r/R (%)*	*(RPM)*	*(W)*	*(dBA)*	*r/R (%)*	*(dBA)*	*(%)*
TE_SSSD_90	0.06	0.13	90	5836	30.4	118	0.81	0.7	0.33
TE_SSDD_90	0.06	0.25	90	5922	31.6	115.4	0.78	3.3	4.29
TE_DSDD_90	0.12	0.25	90	6032	32.2	111.7	0.77	7.0	6.27
TE_SSSD_95	0.06	0.13	95	5813	30.5	117.1	0.79	1.6	0.66
TE_DSSD_95	0.12	0.13	95	5875	30.8	114.8	0.79	3.9	1.65
TE_DSDD_95	0.12	0.25	95	5978	31.5	111.5	0.78	7.2	3.96
Stock				5795	30.3	118.7	0.81		

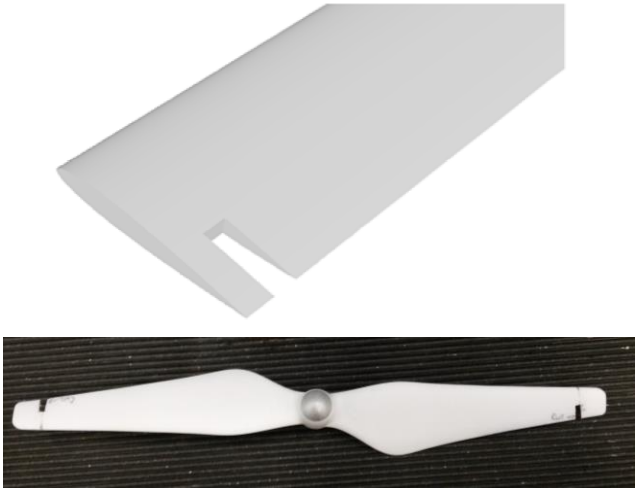

FIGURE 6 TOP- JIN ET AL. TRAILING EDGE NOTCH [42]; BOTTOM – DSDD DJI PHANTOM 2 TRAILING EDGE NOTCH CONFIGURATION

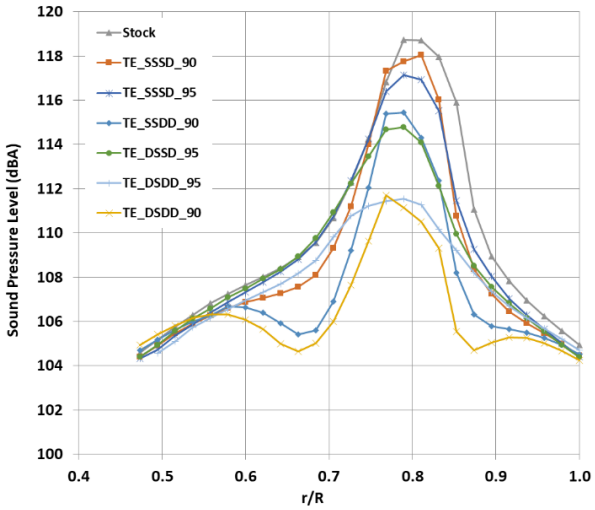

FIGURE 7 SPL VS r/R COMPARISON FOR TE NOTCHES – 1 INCH TRAVERSE

shows only one vortex that is dissipated very quickly downstream

2. Trailing Edge Notches

The study of trailing edge (TE) notches was motivated by a design proposed by Jin et al. [42] shown in Fig. 6. This design was a rectangular TE notch near the wing tip, which they referred to as a chipped wing, that could significantly reduce the wing tip vortex generated during takeoff and landing. When cruising, the notch could be covered to reduce drag. An aspect ratio of 5 was the most effective notch. While the study sought to optimize the notch and understand what parameters were important, it was not concerned with noise generation. Similar findings were presented by Zouaoui et al. [43] however, they considered substantially larger notches more inboard of the wing. Their work lowered vorticity using optimized wing notches and an ogee tip compared to a previous notched configuration.

Following the guidance from Jin et al. and knowing the results of the LE notches, it was decided to test TE notches at an r/R of 0.90 and 0.95. A modified propeller is shown in Fig. 6. Single and double slot width values as well as single and double depth vales are:

1. Single Slot width (SS)– 0.06 inch wide
2. Double Slot width (DS) – 0.12 inches wide
3. Single Depth (SD)– 0.13 inches
4. Double Depth (DD) – 0.25 inches

Table 2 lists the configurations tested and the data collected for each configuration compared to the stock propeller. Figure 7 shows the 1 inch traverse for all TE

TABLE 3 HOLE CONFIGURATIONS AND DATA - TESTED AT 0.7 LB_F

Description	Hole Dia	Hole location	Rotational Speed	Mechanical Power	Peak SPL	Peak SPL Location	SPL decrease	Power increase
	(in)	*r/R (%)*	*(RPM)*	*(W)*	*(dBA)*	*r/R (%)*	*(dBA)*	*(%)*
H_SD_97	0.054	97	5691	32	119.2	0.86	-2	-2.14
H_DD_97	0.090	97	5665	31.9	116.5	0.82	0.7	-2.45
H_TD_97	0.125	97	5680	31.4	115.5	0.82	1.7	-3.98
H_SD_95	0.054	95	5697	31.6	118.6	0.82	-1.4	-3.36
H_DD_95	0.090	95	5729	33.1	114.2	0.8	3	1.22
H_TD_95	0.125	95	5871	34.5	112	0.77	5.2	5.50
H_SD_90	0.054	90	5829	33	118.9	0.84	-1.7	0.92
H_DD_90	0.090	90	5829	34.5	113.6	0.79	3.6	5.50
H_TD_90	0.125	90	5905	36.3	110.7	0.78	6.5	11.01
stock			5585	32.7	117.2	0.84		

FIGURE 8 DEVELOPMENT OF TIP VORTICIES AND THE SHEAR LAYER FOR THE TRAILING EDGE NOTCH

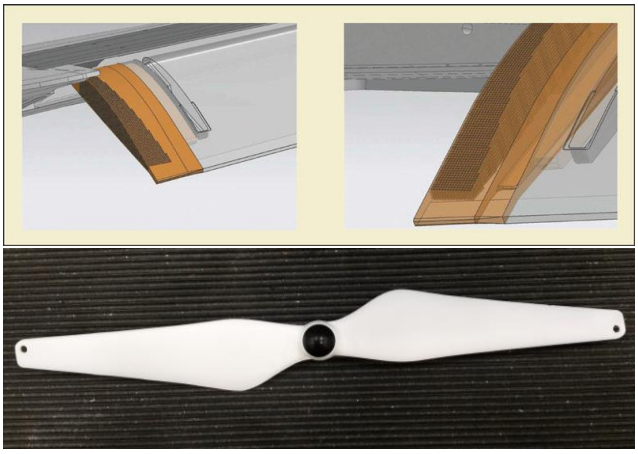

FIGURE 9 TOP- RIGID OPEN LATTICE TREATMENT OF FLAP EDGE [44]; BOTTOM –DJI PHANTOM 2 HOLE CONFIGURATION

notch configurations tested. The location of the peak SPL tends slightly toward the hub as TE notches are introduced to the propeller. The Single Slot width Single Depth (SSSD) configurations had the smallest drop in SPL and the smallest increase in power required. The best configurations for SPL reduction were the Double Slot Double Depth (DSDD) modifications. ***Of the two, the r/R of 0.95 which reduced the SPL 7.2 dBA with an increase in power required of only 3.96% over the stock propeller was the best.***

Figure 8 shows, for the TE notch, the smoke visualization of the vortex generation at the tip. The TE notch shows two small vortices being generated, one at the tip and one at the notch. Both vortices coalesce in a short distance downstream which quickly dissipates the vortices.

3. Holes

Motivation for this tip treatment was found in the December 2107 NASA Tech Briefs [44]. They proposed a modification to a flap edge that was a rigid, open lattice (honeycomb-like) and fin structure to delay the formation of a noise-generating vortex at the flap side edge as shown in Fig. 9. The pressure differential was allowed to communicate through the perforations reducing the driving potential for vortex formation. The result claimed is a 3-5 dBA reduction in noise. Applications envisioned by NASA are helicopter blade tips, gas turbine fan blade tips as well as wind turbine tips. No mention was made of additional drag incurred by this modification.

To test this tip treatment, stock propellers were modified propellers at an r/R of 0.90, 0.95, and 0.97 with three hole diameters, 0.054, 0.090, and 0.125 inches, similar to what is shown in Fig. 9. Table 3 lists the configurations tested and the data collected for each configuration compared to the stock propeller. Figure 10 shows the 1 inch traverse

TABLE 4 VORTEX GENERATOR CONFIGURATIONS AND DATA - TESTED AT 0.7 LB_F

Description	Height	Angle	VG TE location	Rotational Speed	Mechanical Power	Peak SPL	Peak SPL Location	SPL decrease	Power increase
	(in)	*(deg)*	*(in)*	*(RPM)*	*(W)*	*(dBA)*	*r/R (%)*	*(dBA)*	*(%)*
VG_FH_0_0.5	0.20	0	0.50	5961	34.5	116.3	0.82	3.70	9.18
VG_FH_15_0.5	0.20	15	0.50	6042	37.7	112.4	0.80	7.60	19.30
VG_FH_30_0.5	0.20	30	0.50	6444	42.3	108.6	0.80	11.40	33.86
VG_HH_30_0.5	0.10	30	0.50	6244	39.9	109.5	0.79	10.50	26.27
VG_TH_30_0.5	0.05	30	0.50	5690	32.7	114.6	0.80	5.40	3.48
VG_FH_30_0.25	0.20	30	0.25	6134	40.5	110.7	0.77	9.30	28.16
VG_HH_30_0.25	0.10	30	0.25	5950	35.5	111.7	0.77	8.30	12.34
Stock				5781	31.6	120	0.80		

data for all hole configurations tested. The location of the peak SPL tends toward the hub as the hole diameters are increased. No radial trend was noted for peak SPL with different r/R locations. In general, moving the hole further from the tip decreased the peak SPL when compared to the stock propeller. Also, increasing the hole diameter tended to decrease the peak SPL. The measurements with the smallest diameter were actually slightly nosier than the stock propeller and resulted in slightly less power required. The r/R of 0.90 with the 0.125 inch diameter hole was the quietest propeller tested being 6.5 dBA lower resulting in an 11.01% required power increase. ***The acceptable tradeoff might be to use the r/R 0.95 value with the largest diameter which lowers the SPL 5.2 dBA while only requiring a 5.5% increase in power required.***

No smoke visualization was accomplished for the hole configuration.

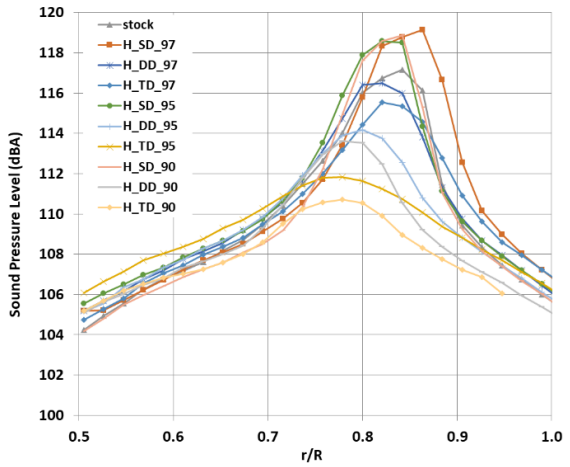

FIGURE 10 SPL VS r/R COMPARISON FOR HOLES – 1 INCH TRAVERSE

4. Vortex Generators

The value of vortex generators (VG) for control of boundary layer separation is well known. Vortex generators can be seen on many commercial aircraft wings to trip the boundary layer to turbulent flow, energizing the boundary layer, especially at higher angles of attack. Heyes and Smith [45] proposed to use a vortex generator to modify the wing tip vortex, as shown in Fig. 11, reducing the wake hazard associated with large commercial aircraft. They tested several sizes, shapes and locations of VGs near the wing tip to determine the influence of the VG on the formation of the wing tip vortex. They found that co-rotating VGs merged with the tip vortex and increased its size. It was difficult to generate a counter-rotating vortex due to the tip airflow. While their study was inconclusive for a propeller application, it was decided to examine VGs on propeller tips. Kim et al [46] tested the influence of VGs that were located with the TE of the VG 0.5 inches from the tip at angles of 0, 15, and 30 degrees with respect to the LE. The VG was 0.5 inches long, 0.2 inches in height with a 45 degree sweep at the leading edge. Three different heights were tested, 0.2, 0.1, and 0.05 inches. A further test was accomplished for the 30 degree configuration with the TE 0.25 inches from the tip. Two different heights were tested at this configuration.

Table 4 lists the configurations tested and the data collected for each configuration compared to the stock propeller. For the configuration with the TE of the VG 0.5 inches from the tip, the 30 degree full height VG reduced the SPL the most, 11.4 dBA, with a 33.86% increase in required power. For the 30 degree half height the SPL decreased 10.5 dBA with a 26.27 % increase in power which might be more acceptable. Moving the VG closer to the tip did not decrease SPL more than at the previous location, however, the power required also decreased accordingly. Decreasing the height of the VG resulted in a smaller SPL decrease and reduced power required. ***A final choice for the VG configurations could be the 0.25 inch TE with a 30 degree angle and a half height VG. This***

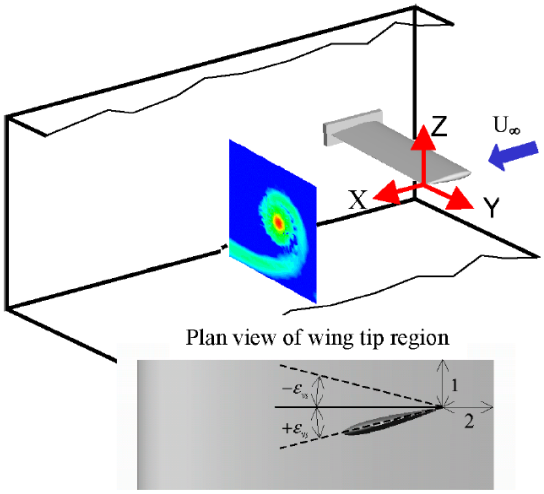

FIGURE 11 TOP- HEYES AND SMITH VORTEX GENERATORS [46]; BOTTOM –DJI PHANTOM 2 VORTEX GENERATOR CONFIGURATION

resulted in an 8.3 dBA decrease in SPL with only a 12.34% increase in required power.

Figure 12 shows the 1 inch traverse for all VG configurations tested. The location of the peak SPL tends toward the hub as the VG moved to the tip. No radial trend was noted for peak SPL location with changes in height.

Figure 13 clearly shows the vortex generator is effective at reducing the tip vortex however, the cost in power is rather large.

5. Tip Thread

Lee et al. [47] suggests that attaching a flexible thread to the tip of a propeller could attenuate the tip vortex from being generated as is shown in Fig. 14. This study was conducted in a water tunnel and the application was for navy ship propellers. They studied the flexible thread with an elliptical wing tip to see if the technique would reduce cavitation. The conclusion was that the flexible thread at the wing tip led to a noticeable reduction in the streamwise velocity field, resulting in the alleviation of the tip vortex and cavitation. This seemed promising so a thin thread, from the core of a parachute cord, was glued to the tip of a stock propeller using superglue. The thread was 1 1/8 inches long and a tiny bit of super glue was put on the tip of the cord to keep it from fraying. This long cord was tested and then it was reduced by ½ inch and tested again. The modified propeller can be seen in Fig. 14.

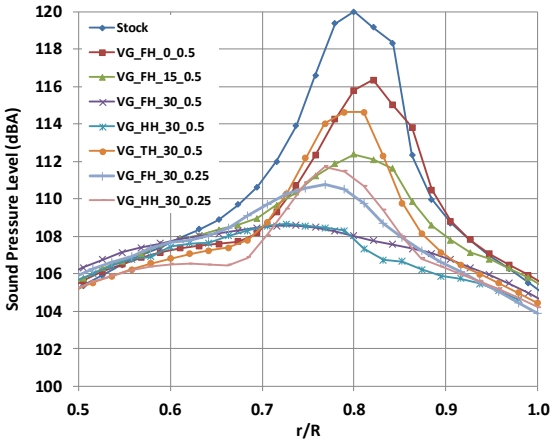

FIGURE 12 SPL VS r/R COMPARISON FOR VORTEX GENERATORS – 1 INCH TRAVERSE

FIGURE 13 DEVELOPMENT OF TIP VORTICIES AND THE SHEAR LAYER ON THE PROPELLER IN THE VORTEX GENERATOR CONFIGUATION

Table 5 lists the configurations tested and the data collected for each configuration compared to the stock propeller. For the tip string, it is interesting to note that each configuration has the same RPM however, as no modification was made to the surface area of the stock propeller, this seems reasonable. ***The long tip string was relatively effective at reducing the SPL with a value of 7 dBA, however, the increase in required power of 47.85% is unacceptable.*** Reducing the string length by ½ inch resulted in a significant change in the SPL, a drop of only 2.2 dBA with a corresponding decrease in power required to only 21.78% above the stock propeller. ***For comparison purposes, the long string length will be used as the best configuration as it is on the order of the other SPL decreases.***

Figure 15 shows the 1 inch traverse for all tip string configurations tested. The radial location of the peak SPL tends toward the hub as the string length was shorter.

Figure 16 clearly shows that for the half string, the vortex is not as influenced by the flexible thread as the vortices are seen downstream of the propeller blade. A 7

TABLE 5 TIP STRING CONFIGURATIONS AND DATA - TESTED AT 0.7 LB_F

Description	String Length	Rotational Speed	Mechanical Power	Peak SPL	Peak SPL Location	SPL decrease	Power increase
	(in)	*(RPM)*	*(W)*	*(dBA)*	*r/R (%)*	*(dBA)*	*(%)*
String_FL	1.125	5955	44.8	111.7	0.81	7.00	47.85
String_HL	0.625	5955	36.9	116.5	0.79	2.20	21.78
stock		5799	30.3	118.7	0.80		

TABLE 6 SAWTOOTH CONFIGURATION AND DATA - TESTED AT 0.7 LB_F

Description	Rotational Speed	Mechanical Power	Peak SPL	Peak SPL Location	SPL decrease	Power increase
	(RPM)	*(W)*	*(dBA)*	*r/R (%)*	*(dBA)*	*(%)*
sawtooth	5866	35.4	113.7	0.79	5.00	16.83
stock	5799	30.3	118.7	0.80		

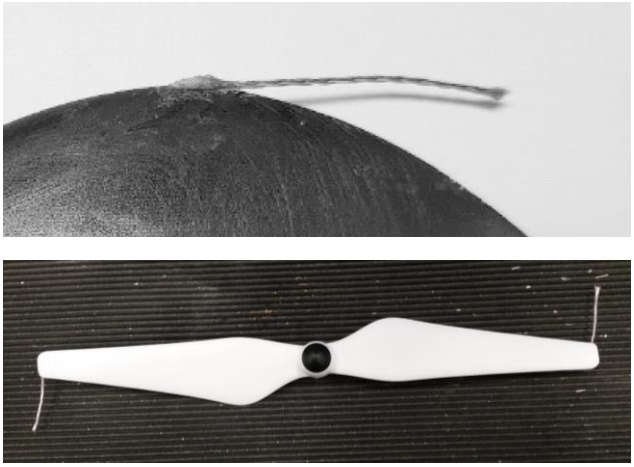

FIGURE 14 TOP- LEE ET AL. FLEXIBLE THREAD [47]; BOTTOM – DSDD DJI PHANTOM 2 FLEXIBLE THREAD CONFIGURATION

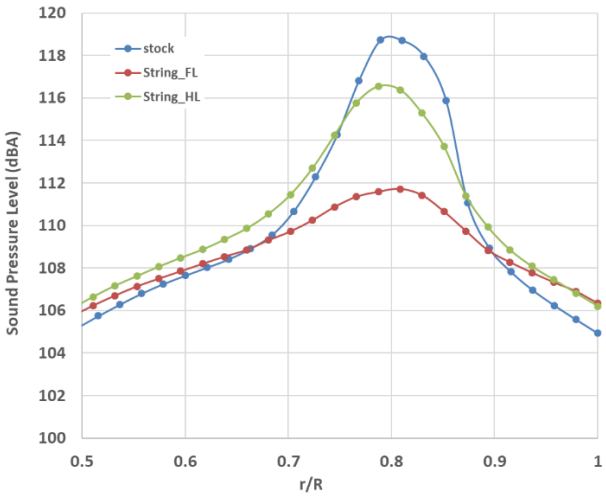

FIGURE 15 SPL VS r/R COMPARISON FOR TIP THREAD LENGTHS – 1 INCH TRAVERSE

dBA decrease in SPL was achieved but at a significant increase in power required. Figure 16 shows that the threads are not as influenced by the air as they would be in the water as found by Lee et al. In the air case, the centrifugal force was greater than the hydrodynamic force experienced by Lee et al. so a substantial increase in power was required in these experiments to overcome the positon of the string which can be seen in the Fig. 16.

6. TE Sawtooth

The motivation for this tip technique was to provide a sawtooth which could produce a vortex that would counter the propeller tip vortex. For standard wings, a sawtooth would normally be positioned on the leading edge and would create a vortex which would flow over the wing and act like a wing fence to prevent tipwise flow. Studies show using a sawtooth on the trailing edge of airfoils, as shown in Fig. 17 [48], reduces noise generation. For this test it was desired to create a vortex to counter the propeller tip vortex. Since the TE notch was so successful, it was decided to place the sawtooth on the trailing edge. Only one configuration was tested. This configuration, shown in Fig. 17, had the tip of the sawtooth at an r/R of 0.95. It extended ¼ inch out from the TE of the propeller at this location and tapered on a diagonal to the tip. The sawtooth was fabricated from 1/8 inch balsa wood which was extended with a 1/8 inch tab on the top and bottom of the

TABLE 7 REVERSE HALF DELTA CONFIGURATION AND DATA - TESTED AT 0.7 LB_F

Description	Rotational Speed	Mechanical Power	Peak SPL	Peak SPL Location	SPL decrease	Power increase
	(RPM)	*(W)*	*(dBA)*	*r/R (%)*	*(dBA)*	*(%)*
half_delta	6113	32.1	120.7	0.78	-2.0	5.94
stock	5799	30.3	118.7	0.80		

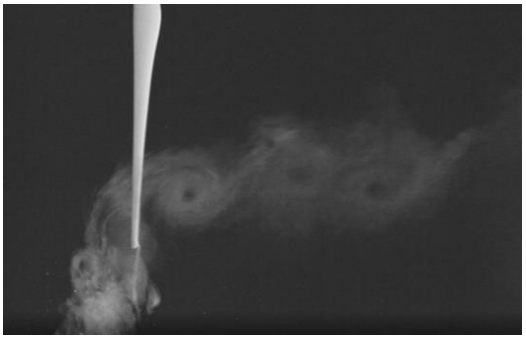

FIGURE 16 DEVELOPMENT OF TIP VORTICIES AND THE SHEAR LAYER ON THE PROPELLER IN THE HALF FLEXIBLE THREAD CONFIGUATION

TE of the propeller. Superglue was then used to fasten the sawtooth to the propeller.

Table 6 lists the configurations tested and the data collected for each configuration compared to the stock propeller. ***Only one configuration was tested and resulted in a 5 dBA decrease for an increase in required power of 16.83%. No additional tests were conducted.***

Figure 18 shows the 1 inch traverse for the sawtooth configuration tested. The location of the peak SPL tends toward the hub with the sawtooth.

No smoke visualization was accomplished for the sawtooth configuration.

7. Reverse Half-Delta

Lee and Su [49], Nikolic [50], and Lee and Nikolic [51] studied the reverse half-delta configuration on a wing tip as seen in Fig. 19. The reverse half-delta configuration is a 65 degree sweep angle from the trailing edge to the LE tip. This creates a sharp LE tip that then tapers toward the TE, removing part of the wing tip resulting in less surface area for the propeller. The stationary reverse half-delta tested on a wing tip by Lee and Su resulted in a weaker wing tip vortex. These research papers also looked at moveable reverse half delta tips that could change angle of attack or that contained moveable strakes. Since this was impractical for a propeller tip, only the stationary reverse half-delta was tested. Table 7 lists the data for the reverse half delta configuration tested, shown in Fig. 19, and the data collected compared to the stock propeller***: Only one***

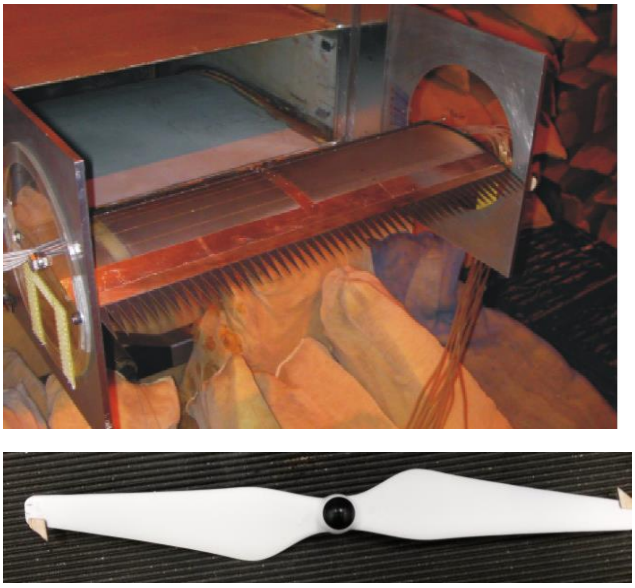

FIGURE 17 GRUBER ET AL. SAWTOOTH [48]; BOTTOM – DSDD DJI PHANTOM 2 SAWTOOTH CONFIGURATION

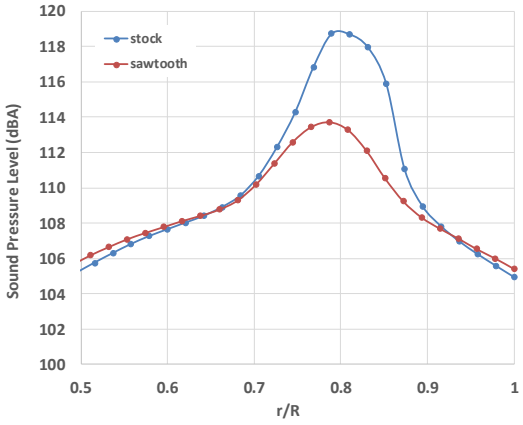

FIGURE 18 SPL VS r/R COMPARISON FOR A SAWTOOTH – 1 INCH TRAVERSE

TABLE 8 SUMMARY OF THE BEST CONFIGURATIONS FOR EACH TIP TREATMENT

Description	Configuration	r/R	Rotational Speed	Mechanical Power	Peak SPL	Peak SPL Location	SPL decrease	Power increase
		(%)	*(RPM)*	*(W)*	*(dBA)*	*r/R (%)*	*(dBA)*	*(%)*
String	FL	100	5955	44.8	111.7	0.81	7.00	47.85
TE	DSDD	95	5978	31.5	111.5	0.78	7.20	3.96
LE	DSDD	90	6148	41.7	110.1	0.77	8.60	37.62
holes	TD	95	5905	36.3	110.7	0.77	8.00	19.80
SAW	SAWTOOTH	95	5866	35.4	113.7	0.79	5.00	16.83
VG	HH_30_0.25		6444	42.3	108.6	0.77	10.10	39.60
Half Delta	Half_Delta		6113	32.1	120.7	0.78	-2.00	5.94
Stock			5799	30.3	118.7	0.80		

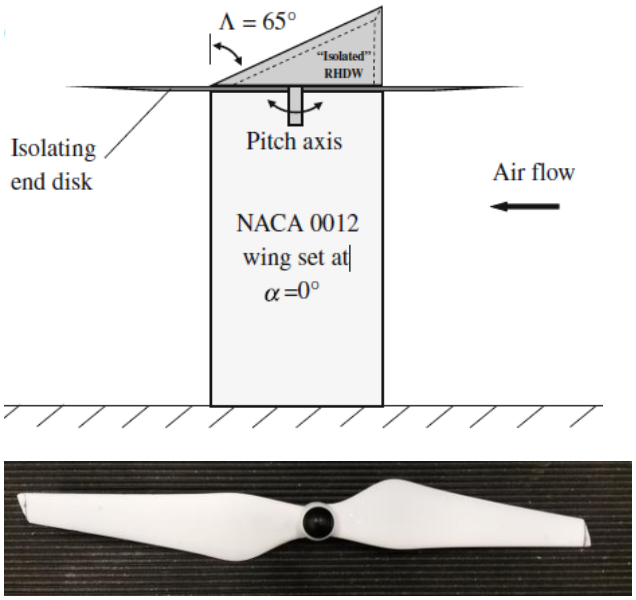

FIGURE 19 LEE AND SU REVERSE HALF DELTA [49]; BOTTOM – DSDD DJI PHANTOM 2 SAWTOOTH CONFIGURATION

configuration was tested and, because of the result of a 2 dBA increase for an increase in required power of 5.94%, no additional tests were conducted.

Figure 20 shows the 1 inch traverse for the reverse half delta configuration tested. The radial location of the peak SPL tends slightly toward the hub with the reverse half delta. Because of the decrease in surface area of the propeller, the RPM increases accordingly to achieve the required thrust which resulted in a higher peak SPL.

No smoke visualization was accomplished for the reverse half-delta configuration.

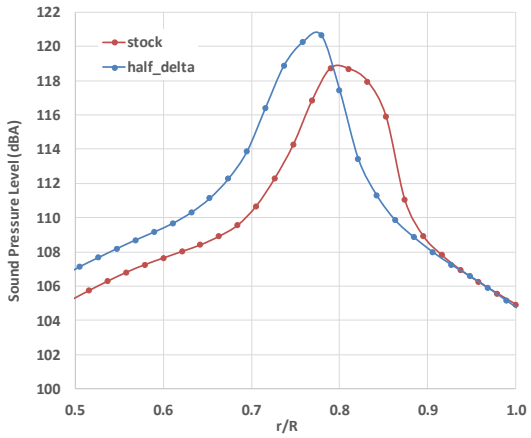

FIGURE 20 SPL VS r/R COMPARISON FOR A REVERSE HALF DELTA – 1 INCH TRAVERSE

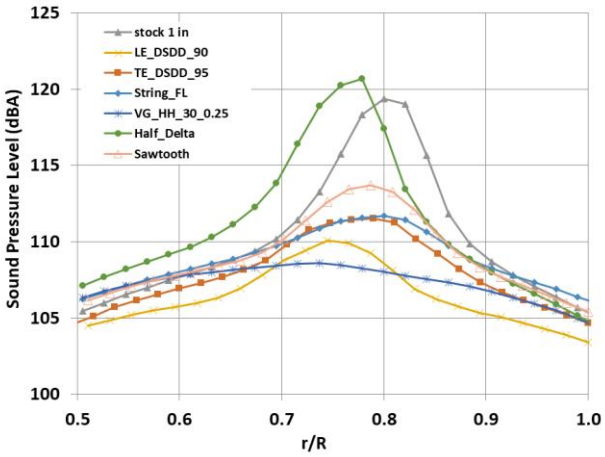

FIGURE 21 SPL VS r/R COMPARISON FOR BEST CONFIGURATIONS TESTED – 1 INCH TRAVERSE

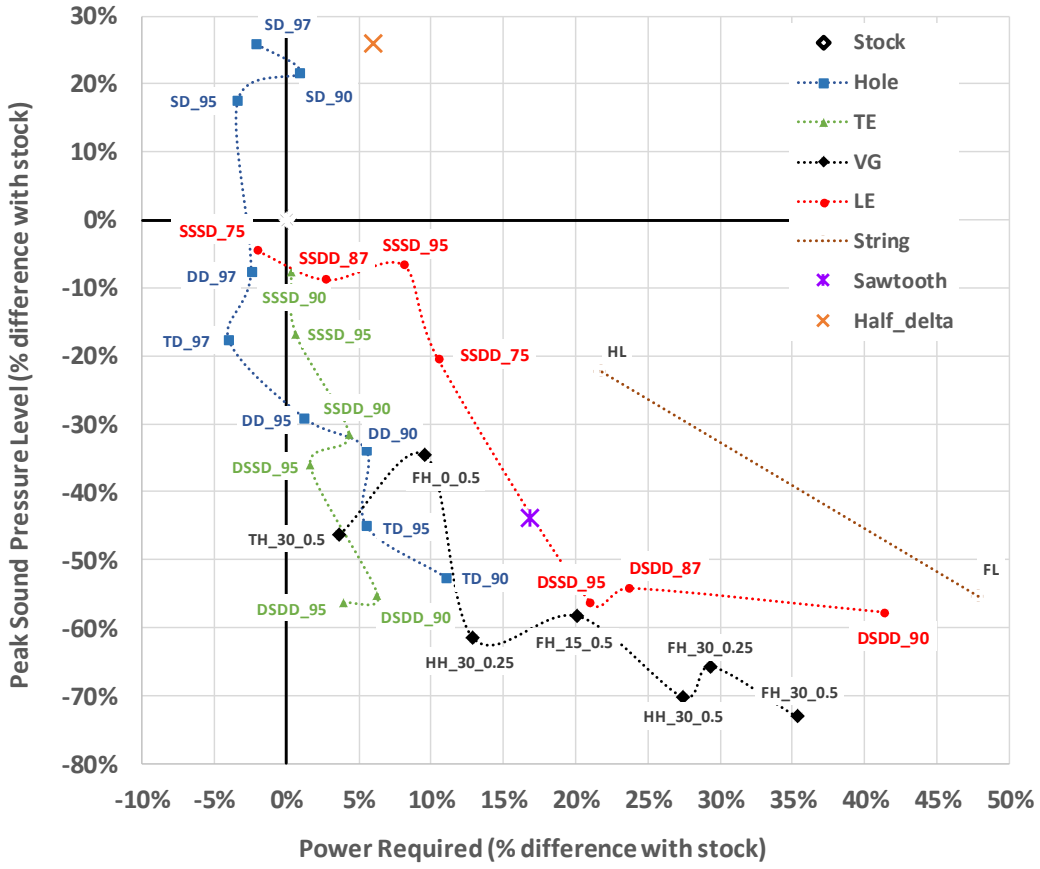

FIGURE 22 INCREASE IN POWER REQUIRED ABOVE THE STOCK PROPELLER AND THE REDUCTION IN SPL FOR THE CONFIGURATIONS TESTED AT 0.7 LB_F THRUST

Summary

Table 8 displays a summary of the best configuration for each of the tip treatments studied. Figure 21 displays the 1 inch traverse for the best configuration for each tip treatment tested. If the goal is to primarily reduce the SPL, at first glance, one might favor the VG 30 full height at the TE 0.5 inch location. This reduces the SPL 10.1 dBA. To get the complete picture one must also consider the increase in power required. In this instance the power required is 39.60% higher than the stock propeller which is unacceptable. The next choice might be the LE 0.9 r/R DSDD configuration which reduces the SPL 8.6 dBA, however this results in an increase in power required of 37.62% which is also unacceptable. The next cluster of configurations show approximately a 7 dBA decrease in SPL. Looking at this group shows the TE 0.95 r/R DSDD drops the SPL 7.2 dBA while only increasing the power required by 3.96%. This configuration seems the most reasonable tradeoff between decreasing SPL for a modest increase in power.

The increase in power required and reduction in SPL are summarized in Figure 22 as a percentage compared with the stock propeller for each tip modification. The configuration for the TE DSDD at the 0.95 r/R location is the recommended configuration from all the configurations tested. This reduces the SPL 56% while only requiring a 3.96 % increase in power required.

FUTURE CONSIDERATION

Bio Inspired

Perhaps the most promising treatments for propellers could come from observing birds in flight. This is called biomimicry and refers to observing the world for inspiration on how to improve any design, the current application being a propeller. Studies on the aerodynamics of birds can be found in the literature [52] which highlights the similarity of a bird's aerodynamic design and its application to aircraft flight. Specific papers can be found which address how to incorporate bio-inspired wing tip devices on aircraft [53]. Many of these tip treatments could be incorporated into a propeller design. One such study by Ning and Hu [54] examined changing the shape of the entire propeller blade planform, including the tip, to

resemble the very similar cicada wing and maple seed. Their findings were that the bio-inspired propeller could generate equal thrust and emit lower noise under a constant power input. A bird's wing tip feathers inspired the proposal by Guerrero et al. [55] to use a biomimetic spiroid winglet to control lift and drag of an aircraft. This tip treatment was successfully applied to a propulsor for a propfan with excellent results [56]. One of the quietest birds known to man is the owl. Studies of the owl's flight will provide numerous biomimetic ideas for the entire wing/propeller system for years to come [57]. Other bio-inspired ideas that could apply to the entire propeller blade might be leading and trailing edge serrations that are observed with bird feathers [58-61].

Custom Designed Propellers with Additional Tip/Blade Treatments

While the focus of these tip treatment modifications was a stock DJI Phantom 2 quadcopter propeller, any of these proposed modifications to either the propeller tip or blade could be applied to the custom propellers designed previously studied by the USAF Academy and Baylor University.

CONCLUSIONS

The focus of this study was to lower the near field SPL of a DJI Phantom 2 quadcopter propeller with a minimum increase in power consumption. Of the tip treatments tested the TE 0.95 r/R DSDD dropped the SPL 7.2 dBA while only increasing the power required by 3.96%. This would seem an acceptable tradeoff. The next step would be to equip a DJI Phantom 2 with four modified propellers and compare the total power consumption and far field noise signature to the quadcopter operating with four stock propellers. There are two questions that have yet to be fully answered. The first question asks what is the maximum allowable SPL for the flight of a quadcopter in a populated urban environment or in an ISR capacity? Callender states that there are currently no regulations for UAS SPLs in the National Air Space System [62]. Clearly this must be addressed in the future. The second question asks what is an acceptable increase in power consumption for a decrease in SPL? More studies similar to those presented in this paper are necessary to address this question. Both of these questions should be explored in the pursuit of the quiet but efficient propeller for a quadcopter application.

NOMENCLATURE

B&K	Brüel & Kjær
dBA	A-Weighted Sound Pressure Level
D	Distance from the hub
D_1	Distance to the first measured SPL for a radial line
ISR	Intelligence, surveillance, and reconnaissance
p	Pressure being measured
p_0	Reference sound pressure 20 μPa
r	Distance from hub to location on the propeller blade
R	Distance from hub to tip of propeller
RPM	Revolutions per minute
SPL	Sound Pressure Level
UAS	Unmanned Aerial System

REFERENCES

[1] Bruno, M. 2018, "Aerospace Sector Could See Overhaul from Electric Propulsion," Aviation Week & Space Technology Online, http://aviationweek.com/future-aerospace/aerospace-sector-could-see-overhaul-electric-propulsion , August 24, 2018 accessed on January 13, 2019.

[2] Miller, B., 2016, "Will Jet Aircraft of the Future be Powered by Electricity?" http://www.govtech.com/fs/Will-Jet-Aircraft-of-the-Future-be-Powered-by-electricity accessed on October 2, 2017.

[3] NASA, 2015, "LEAPTech to Demonstrate Electric Propulsion Technologies," https://www.nasa.gov/centers/armstrong/Features/leaptech.html accessed on October 3, 2017

[4] Warwick, G., 2016, "The Week in Technology, Oct. 2-6, 2017," Aviation Week and Space Technology Online, http://aviationweek.com/technology/week-technology-oct-2-6-2017 accessed on January 13, 2019.

[5] Slack, M., 2015,"Game of Drones," Science and Technology, Trial, Dec 2015, pp 16-20.

[6] DJI Phantom 2, https://www.dji.com/phantom-2 accessed on January 13, 2019.

[7] Gupte, S., Mohandas, P., Conrad, J., 2012, "A Survey of Quadcopter Unmanned Aerial Vehicles," Southeastcon, 2012 Proceedings of IEEE, Orlando, FL, March 15-18, 2012, pp 1-6, ISBN 978-1-4673-1375-9/12, DOI: 10.1109/SECon.2012.6196930.

[8] Kauntama, E., Cracium, D. Tarca, I., and Tarca. R., 2016, "Quadcopter Propeller Design and Performance Analysis," Joint International conference of the 12th International conference on Mechanism and Mechanical Transmissions, MTM2016, and the 23rd International Conference on Robotics, Achen, Germany, October 26-27, 2016.

[9] Misiunas, M., Skvireckas, R., and Volkovas,V., 2015, "Analysis of the Quadcopter's Noise," 19th International Scientific Conference on Transport Means, Kaunas University of Technology, Kaunas, Lithuania, October 22-23, 2015

[10] Intaratep, N., Alexander, W., Dervenport, W., Grace, S., and Dropkin, a., 2016, "Experimental Study of Quadcopter Acoustics and Performance at Static Thrust conditions," 22nd AIAA/XWAS Aeroacoustics Conference, Lyon, France, May 30 – June 1, 2016.

[11] Aleksandrov, D., and Penkov, I., 2012, "Optimal Gap Distance Between Rotors of Mini Quadcopter Helicopter,"

8th International DAAAM Baltic Conference, Tallinn, Estonia, 19-21 April 2012
[12] Naidoo, Y., Stopforth, R., and Bright, G., 2011, "Rotor Aerodynamic Analysis of a Quadcopter for Thrust Critical Applications," 4th Robotics and Mechatronics Conference of South Africa (ROBMECH 2011), CSIR Pretoria, South Africa, 23-25 November 2011.
[13]Wisniewski, C. F., Byerley, A. R., Heiser, W. H., Van Treuren, K. W., Liller, W. R.., and Wisniewski, N., "Experimental Evaluation of Open Propeller Aerodynamic performance and Aero-acoustic Behavior," AIAA 33 Applied Aerodynamics Conference, Dallas, TX, June 22-26, 2015.
[14] Wisniewski, C. F., Byerley, A. R., Heiser, W. H., Van Treuren, K. W., and Liller, W. R., "Designing Small Propellers for Optimum Efficiency and Low Noise Footprint," AIAA 33 Applied Aerodynamics Conference, Dallas, TX, June 22-26, 2015.
[15] Wisniewski, C. F., Byerley, A. R., Heiser, W. H., Van Treuren, K. W., and Liller, W. R., "The Influence of Airfoil Shape, Tip Geometry, Reynolds Number and Chord Length on Small Propeller Performance and Noise," AIAA 33 Applied Aerodynamics Conference, Dallas, TX, June 22-26, 2015.
[16] Van Treuren, K. W., Hays, A., W., Wisniewski, C. F., and Byerley, A. R.., 2017, "A Comparison of the Aerodynamic Performance and Aeroacoustic Behavior of Commercial and Custom Designed Quadcopter Propellers," AIAA SciTech 2017, Grapevine, TX , January 9-13, 2017.
[17] Wisniewski, C. F., Byerley, A. R.., Van Treuren, K. W., and Hays, A. W., 2017, "Experimentally Testing Commercial and Custom Designed Quadcopter Propeller Static Performance and Noise Generation," AIAA 35 Applied Aerodynamics Conference, Denver, CO , June 5-9, 2017.
[18] Carvvalho, I., "Low Reynolds Propellers for Increased Quadcopters Endurance," Master's Thesis, Universidade Da Beria Interior, October 2013.
[19] Nelson, J. T., 2005, "Practical Modifications for low Reynolds Number Propellers," Master's degree, Wichita State.
[20] Kloet, N., Watkins, S., and Clothier, R., 2017, "Acoustic Signature Measurement of Small Multi-Rotor Unmanned Aircraft Systems," International Journal of Micro Air Vehicles, 9 (1), pp 3-14.
[21] Zhou, W., Ning, Z., Li, H., and Hu, H., 2017, "An Experimental Investigation on Rotor-to-Rotor Interactions of Small UAV," 2017 AIAA Aviation Forum, 35th AIAA Applied Aerodynamics Conference, 3-9 June 2017, Denver, Colorado.
[22] Zhou, T., and Fattah, R., 2017, "Tonal Noise Characteristics of Two Small-Scale Propellers," 2017 AIAA Aviation Forum, 35th AIAA Applied Aerodynamics Conference, 3-9 June 2017, Denver, Colorado.
[23] Deters, R., Kleinke, S., and Selig, M., 2017, "Static Testing of Propulsion Elements for Small Multirole Unmanned Aerial Vehicles," 2017 Aviation Forum, 35th AIAA Applied Aerodynamics Conference, Denver, Colorado, 3-9 June 2017.
[24] Deters, R., Dantsker, O., Kleinke, S., Norman, N., and Selig, M., 2018, "Static Performance Results of Propellers Used on Nano, Micro, and Mini Quadrotors," 2018 Aviation Forum, 2018 Applied Aerodynamics Conference, Atlanta, Georgia, 25-29 June 2018.
[25] Sinibaldi, G., and Marino, L., 2013, "Experimental Analysis on the Noise of Propellers for Small UAV," Applied Acoustics, 74, pp. 79-88.
[26] Leslie, A., Wong, K., and Auld, D., 2010, "Experimental Analysis of the Radiated Noise from a Small Propeller," Proceedings of the 20th International Conference on Acoustics, ICA 2010, Sydney, Australia, 23-27 August 2010.
[27] Leslie, A., Wong, K., and Auld, D., 2008, "Broadband Noise Reduction from a Mini-UAV Propeller Through Boundary Layer Tripping," Acoustics 2008, Geelong, Victoria, Australia, 24-26 November 2008.
[28] Van Treuren, K. W., Wisnieswski, C., and Cinnamon, E., 2018, "Near and Far Field Noise Decay From a Quadcopter Propeller With and Without a Leading Edge Notch," GT2018-75973, Proceedings of ASME Turbo Expo 2018, Turbine Technical Conference and Exposition IGTI2018, Oslo, Norway, June 11 – 15, 2018
[29] Jacquin, L., 2005, "Aircraft Trailing Vortices: an Introduction," C. R. Physique, 6, pp. 395-398.
[30] Karakus, c., Akilli, H., and Sahin, B., 2008, "Formation, Structure, and Development of Wing Tip Vortices," Proc. IMechE, Vol. 222, Part G: Journal of Aerospace Engineering, pp 13-22.
[31] Lombardi, G., and Skinner, P., 2005, "Wing-Tip Vortex in the Near Field: An Experimental Study," Journal of Aircraft, 42 (5), September-October 2005, pp. 1366-1368.
[32] Birch, D., Lee, T., Mokhtarian, F., and Kafyeke, F., 2003, "Rollup and Near-Field Behavior of a Tip Vortex," Journal of Aircraft, 40(3), pp. 603-607.
[33] Craft, T., Gerasimov, A., Launder, B., and Robinson, C., 2006, "A Computational Study of the Near-Field Generation and Decay of Wingtip Vortices," International Journal of Heat and Fluid Flow, 27, pp 684-695.
[34] Feder, D., Dhone, M., Kornev, N., and Abdel-Maksoud, M., 2018, "Comparison of Different Approaches Tracking a Wing Tip Vortex," Ocean Engineering, 147, pp. 609-675.
[35] Giuni, M., and Green, R., 2013, "Vortex Formation on Squared and Rounded Tip," Aerospace Science and Technology, 29, pp 191-198.
[36] Bailey, S., Tavoularis, S., and Lee, B., 2006, "Effects of Freestream Turbulence on Wing Tip Vortex Formation

and Near Field," Journal of Aircraft, 43(5), September-October 2006.
[37] Savas, O., 2005, "Experimental Investigation on Wake Vortices and Their Alleviation," C. R. Physique, 6, pp 415-429.
[38] Ning, A. and Kroo, I., 2010, "Multidisciplinary Conservations in the Design of Wings and Wing Tip Devices," Journal of Aircraft, 47(2), March-April 2010.
[39] Sohon, M., and Chang, J., 2012, "Visualization and PIV Study of Wing-Tip Vortices for Three Different Configurations," Aerospace Science and Technology, 16, pp. 40-46.
[40] Kline, S. J., and F. A. McClintock: "Describing Uncertainties in Single-Sample Experiments", Mech. Eng., p. 3, January 1953
[41] Demoret, A., and Wisniewski, C., 2018, "The Impact of a Notched Leading Edge on Performance and Noise Signature of Unmanned Aerial Vehicle Propellers," AIAA Region V Student Conference, Saint Louis University, Saint Louis, MO, April 13-14, 2018.
[42] Jin, J., Oh, S., and Yee, K., 2014, "Numerical Simulation of Trailed Vortex Alleviation Through Chipped Wingtip Shapes," Journal of Mechanical Sciences and Technology, 28 (9), pp. 3605-3615.
[43] Zouaoui, Z., Szkatula, L., and Grang, R., 2007, "Computational Analysis of Wake Vortices Generated By Notched Wings," Journal of Aircraft, 44 (2), March-April 2007, pp. 487-500.
[44] NASA Tech Briefs, Langley Research Center, 2017, "Flap Edge Noise Reduction Fins," Tech Briefs, December 2017, p 26.
[45] Heyes, A., and Smith, D., 2005, "Modification of a Wing Tip Vortex by Vortex Generators," Aerospace Science and Technology, 9, pp 469-475.
[46] Kim, T., Kowalkowski, G., and Wisniewski, C., 2018, "Propeller Noise Reduction of Unmanned Aerial Vehicles," Paper presented in fulfilment of AE 471 Laboratory Methods course, USAF Academy, May 2018.
[47] Lee, S., Shin, J., Arndt, R., and Suh, J., 2018, "Attenuation of the Tip Vortex Using a Flexible Thread," Experiments in Fluids, 59:23. pp 1-12.
[48] Gruber, M., Azarpeyvand, M., and Joseph, P., 2010, "Airfoil Trailing Edge Noise Reduction by the Introduction of Sawtooh and Slitted Trailing Edge Geometries," Proceedings of the 20th International Congress on Acoustics, ICA 2010, 23-27 August 2010.
[49] Lee, T., and Su, Y., 2012, "Wing Vortex Control Via the Use of a Reverse Half-Delta Wing," Exp Fluids, 52, pp. 1593-1609.
[50] Nikolic, V., 2005, "Movable Tip Strakes and Wing Aerodynamics," Journal of Aircraft, 42 (6), November – December 2005, pp. 1418 – 1426.
[51] Lee, T., and Nikolic, V., 2008, "Effects of a Moveable Tip Strake on Wake Vortex Structure," Journal of Aircraft, 45 (4), July-August 2008, pp. 1305-1314.
[52] Dvorak, R., 2016, "Aerodynamics of Bird Flight," EPJ Web of Conferences, 114, pp. 1-8.
[53] Lynch, M., Mandadzhiev, B., and Wissa, A., 2018, "Bioinspired Wingtip Devices: A Pathway to Improve Aerodynamic Performance During Low Reynolds Number Flight," Bioinspired Biomimicry, 13, pp. 1-14.
[54] Ning, Z, and Hu, H., 2017, "An Experimental Study on the Aerodynamic and Aeroacoustic Performances of a Bio-Inspired UAV Propeller," 2017 Aviation Forum, 35th AIAA Applied Aerodynamic Conference, Denver, Colorado, 5-9 June 2017.
[55] Guerrero, J., Maestro, D., Bottaro, and Bottaro, A., 2012, "Biomimetic Spiroid Winglets for Lift and Drag Control," C. R. Mercanique, 340, pp. 67-80.
[56] Patrao, A., "Innovative Propulsors and Engine Integration," Presentation from the Chalmers University of Technology.
[57] Wagner, H., Weger, M., Klaas, M., and Wolfgang Schroder, W., 2018, "Features of the Owl Wings That Promote Silent Flight," Interface Focus, 7, pp. 1-11.
[58] Drovetski, S., 1996, "Influence of Trailing Edge Notch on Flight Performance of Galiforms," The Auk, 113 (4), October 1966, pp 802-810.
[59] Ning, Z., and Hu, 2017, "An Experimental Study on the Aerodynamics and Aereoacoustic Characteristics of Small Propellers," 2017 Aviation Forum, 35th AIAA Applied Aerodynamic Conference, Denver, Colorado, 5-9 June 2017.
[60] Chong, T., Vayhylakis, A., McEwen, A, Kemsley, F., Muhammad, C., and Siddiqi, S., Aeroacoustic and Aerodynamic Performances of an Aerofoil Subjected to Sinusoidal Leading Edges," AIAA
[61] Ning, Z., Wlezien, R., and Hu, H., 2017, "An Experimental Study on Small UAV Propellers with Serrated Trailing Edges," 2017 Aviation Forum, 35th AIAA Applied Aerodynamic Conference, Denver, Colorado, 5-9 June 2017.
[62] Callender, M. N., 2018, "UAS Propeller /Rotor Sound Pressure Level Reduction Through Leading Edge, Upper Surface, and Trailing Edge Modifications," AUVSI XPONENTIAL, Denver, CO, April 30 – May 3.